CHAPTER 1

INTRODUCTION

1.1. Gas-liquid-solid reaction systems.

Three-phase reactors are widely used in chemical process industry. Hydrogenation, oxidation and hydration are often carried out on a solid catalyst in three-phase reaction systems. In some three-phase reaction systems, e.g. in coal liquefaction, the solid is a reactant. Sometimes, one of the three phases is an inert medium which improves heat and mass transfer.
The gas-liquid-solid reactions are carried out in a column or a vessel which contains all three phases.
Three types of gas-liquid-solid reactions can be distinguished:

(1) reactions where gas, liquid and solid are either reactant or product. The absorption of carbon dioxide in a suspension of lime to produce an aqueous solution of calcium carbonate and the thermal liquefaction of coal are examples of this type of reaction.

(2) gas-liquid-solid reactions in which the solid acts as a catalyst for the gas-liquid reaction. This type of a three-phase reaction system is often encountered in the chemical process industry. Not only reactants are absorbed from the gas phase but volatile products can be desorbed as well. Furthermore, there could be reaction systems, e.g. the catalytic liquefaction of coal, in which the solid phase is both a reactant and a catalyst.

(3) gas-liquid-solid reactions in which components from two phases react with each other and the third phase is inert. When the solid is inert, reactions are carried out in a fixed bed column. The gas-liquid reaction is often carried out under countercurrent flow conditions. The solid improves in particular the gas-liquid contact and gas-liquid mass transfer. When the liquid is the inert phase, it is used as a medium for heat transfer or for redistribution of the concentrations of the reactants or products at the catalyst surface. In the case that the gas phase is the inert medium, it improves the mixing of the liquid-solid suspension.

Shah [1] gives an extensive list of examples of the above-mentioned types of gas-liquid-solid reaction systems.

1.2. Reactors containing gas-liquid-solid systems.

The reactions in gas-liquid-solid systems are carried out in a number of reactor types which can be divided into two groups:
- fixed bed reactors in which the solid bed is fixed;
- slurry reactors in which the solid phase is suspended in the liquid phase.

In fixed bed reactors the gas and liquid phases can flow:
- countercurrently, with the gas flowing upwards and the liquid flowing downwards;
- cocurrently downwards;
- cocurrently upwards.

In trickle bed reactors, gas and liquid normally flow cocurrently downwards.
A reactor with cocurrent upward flows of gas and liquid in a fixed solid bed is called a packed bubble reactor.
The slurry reactors can be distinguished into:
- mechanically agitated slurry reactors;
- gas-agitated slurry reactors;
- gas-liquid agitated cocurrent upflow fluidized bed reactors.

In mechanically agitated and gas-agitated reactors the influence of the superficial liquid velocity is usually negligible. In Table 1.1. a review of some operation modes of three-phase reactors is given, with a few examples.

1.3. Slurry reactors.
In this thesis the discussion is restricted to gas-liquid-solid reaction systems in which the solid acts as a catalyst and is homogeneously suspended in the liquid. The gas phase is the dispersed phase whereas the liquid is the continuous phase. In particular the subject of mass transfer in a three-phase reaction system with gas agitation is dealt with. Our experiments were carried out with a zero net liquid flowrate. The results of these experiments may be applied to a slurry reactor with a relatively low value of the superficial liquid velocity.
For the design of large-scale industrial slurry reactors, knowledge is required about the hydrodynamic behaviour and the transport properties of the reaction system. Sometimes, knowledge of the properties of the gas-liquid system only is insufficient for a successful design of slurry reactors. It has been found that the suspended solid can have a large influence on gas holdup and bubble size.
In the past two decades a number of investigations have been carried out on both the hydrodynamic and the transport properties in slurry reactors.
Most publications deal with one or more hydrodynamic properties of two or three-phase reaction systems. Publications of interest are mentioned and discussed in Chapter 2 where the hydrodynamic behaviour of two and three-phase bubble columns is treated in more detail.
In a number of articles a theoretical analysis is given of the mass transfer process in slurry systems in which the solid acts as a catalyst. Solutions are given for the effectiveness and the gas absorption rate in slurry systems for chemical reactions of different orders. Further, articles have been published in which the experimental results are given for several hydrodynamic and transport properties focusing on a single system under certain conditions of temperature and pressure.

Kölbel and Hammer et al. published a number of papers in which they discuss the conversion, kinetics and mass transfer of hydrogenation reactions. Kölbel and Maennig [2] discussed the kinetics of the ethylene hydrogenation on Raney nickel suspended in hydrocarbons at 1 bar and at temperatures between 30 and 100 °C. Kölbel, Klötzer and Hammer [3] have investigated the system mentioned at pressures up to 6 bar and have given reactor design rules with which the reactor behaviour at different conditions can be simulated. Kölbel, Matsuura and Hammer [4] described experiments with the hydrogenation of n-dodecene-1 on suspended Raney nickel catalyst at 1 bar as experimental proof of the macro-kinetic reactor design equations with which the reactor performance as a function of operating conditions can be predicted. Identical objectives were pursued by Hammer and Schmal [5] with the hydrogenation of carbon monoxide to methane. Further articles of Kölbel et al. [6,7] deal with the design of slurry reactors. More recently, the development and scale-up of a slurry reactor for the production of hydroxylamine on a commercial scale have been investigated in every detail. Some results of this study and the experience of scale-up of the equipment have been published by Van Dierendonck et al. [8-10] and De Rooij et al. [11].
Other three-phase reaction systems have been investigated on laboratory scale by Gut et al. [12], who reported about the kinetics of the liquid phase hydrogenation and isomerization of sunflower oil with nickel on silica catalyst and by Sadana [13], who performed experiments with the aqueous phase oxidation of maleic acid on supported CuO catalyst. Johnson et al. [14] described the results of the hydrogenation of α-methylstyrene by means of a suspended palladium on alumina catalyst whereas Price and Schiewetz [15] reported about the hydrogenation of cyclohexene in the presence of a supported platinum catalyst. It should be pointed out that most kinetic measurements with small-scale slurry reactors are carried out with mechanical agitation. In large-scale slurry reactors, gas-agitation is preferred.
Also Snijder et al. [16] (hydrogenation of nitrobenzene to aniline in an acetic acid solution) and Littman and Bliss [17] (hydrogenation of toluene) made use of a mechanically agitated reactor for their kinetic studies.

Table 1.1. Review of some operation modes of three-phase reactors.

type of reactor	mode of reactor operation		
	gas	liquid	solid
1. fixed bed reactor			
examples:			
- trickle bed reactor	downwards continuous	downwards	fixed
- bubble flow reactor	upwards dispersed	upwards continuous	fixed
- spray flow reactor	upwards continuous	downwards dispersed	fixed
2. slurry reactor			
examples:			
- mechanically agitated slurry reactor	upwards dispersed	upwards downwards continuous batch-wise	suspended
- gas-agitated slurry reactor	upwards dispersed	upwards downwards continuous batch-wise	suspended
- fluidized bed reactor	upwards dispersed	upwards continuous	suspended

Sherwood and Farkas [18] used a gas-agitated slurry reactor for their study on the hydrogenation of α-methylstyrene, the hydrogenation of ethylene using catalyst suspended in oil and the hydrogenation of cyclohexene by catalyst suspended in water.
Slesser et al. [19] investigated some of the parameters affecting the transfer rates in a bubble column by means of the hydrogenation of ethylene with Raney nickel catalyst in an o-xylene medium.
Lefers et al. [20], Kars et al. [21] and Janssen and Joosten [22] searched for the influence of the presence of solid particles on some of the mass transfer properties.
The above-mentioned publications give information on the kinetics of and mass transfer in several reaction systems in mechanically and gas-agitated reactors. Sometimes, the results are used as support for reactor design of particular reaction systems.

Ramachandran and Chaudhari have published theoretical work on the slurry reactor, its kinetics, overall effectiveness and mass transfer rates [23-25].
A theoretical study on the dynamics of a bubble column slurry reactor has been carried out by Govindarao [26] using an axial dispersion model.
Further theoretical work on the mass transfer in slurry reactors has been done by Gut and Bühlmann [27], by Reuther and Puri [28] and Hsu and Reuther [29].

Recently, publications have been presented by Alper, Wichtendahl, Lohse and Deckwer [30-35] which deal with the chemical enhancement of the gas absorption from the gas phase into the liquid phase in slurry systems where the solid acts as a catalyst. These publications are based on a pseudo-homogeneous model for the liquid suspension of catalyst in which very small catalyst particles are in the liquid film. Their main conclusion is that for almost all practical cases of catalytic slurry reactions, the chemical enhancement can be neglected because of the high value of the mass transfer coefficient and the very high concentration of catalyst required to obtain any enhancement.
A review of studies on mass transfer across the gas-liquid interface in three phase slurry systems is given by Østergaard [36].

1.4. Outline of the work to be presented.
The aim of this thesis is to develop reactor design equations for large-scale industrial slurry reactors. The discussion is restricted to the type of gas-agitated slurry reactors in which the liquid is the continuous phase and the gas is the dispersed phase. The gas flows upwards. The solid acts as a catalyst and is suspended homogeneously in the liquid by the gas flow. For the design of slurry reactors it is necessary to have reliable information about:
- the hydrodynamic behaviour of the slurry system;
- the kinetics of the reaction;
- the physical properties of the reaction system, e.g. the transport properties;
- the gas absorption process from the gas phase to the active sites of the catalyst particles.

In this thesis it is shown that it is possible to evaluate reactor design equations from information of separate small-scale experiments on each of the above-mentioned subjects. Combination of the correct information on these subjects leads to reliable reactor design equations.

In Chapter 2 the results of investigations into the hydrodynamic behaviour of a bubble column and a slurry column are discussed. These results relate to:
- the average gas holdup;
- the gas-holdup distribution;
- the solid particle distribution;
- the axial liquid-phase velocity distribution in a cross-section;
- the Sauter mean gas bubble diameter;
- the specific interfacial area.

The experiments were performed in a column (T = 0.29 m, L = 4 m) whose dimensions were chosen so as to make the information obtained representative of a large-scale column.

In Chapter 3 the solubility of gas in the reaction liquid is discussed and a desorption method for the determination of the solubility of slightly soluble gases in liquids is given.

Because of the lack of reliable information on the diffusion coefficient of the gas in the reaction medium, we have developed a new method (Constant Bubble Size method) which leads to accurate and reliable data on the diffusion coefficient of slightly soluble gases in liquids. The theory of the CBS-method, equipment and results of the experiments are presented in Chapter 4.

In Chapter 5 we shall describe some models for the mass transfer of gas from the dispersed gas phase to the active sites of the catalyst particles which are suspended homogeneously in the liquid. We will discuss models in which the catalyst particles are:
- in the bulk of the liquid only;
- in the liquid film only;

- suspended homogeneously in both the bulk of the liquid and the liquid film.

In Chapter 6 the results of the experiments with some three-phase reaction systems are discussed in the light of the theory of Chapter 5. These experiments were carried out in a Whitman cell containing about 1 litre of liquid and about 0.5 litres of gas. The liquid and the gas phase are mechanically stirred separately. The gas-liquid interface is a circular flat horizontal surface with a specific interfacial area of about 9 m^{-1}.

In Chapters 2 to 6 experiments performed in equipment of different scale are described. The experimental results concerning the hydrodynamic behaviour were obtained in a 300 dm^3 slurry column; the chemical reactions were carried out in a 1.5 dm^3 Whitman cell; the diffusion coefficients of the slightly soluble gases in the liquids were obtained in a 3 cm^3 diffusion cell.
Although the experiments concerning gas absorption with chemical reaction in a three-phase reaction system were carried out in a Whitman cell, it is also possible to perform such experiments in the above-mentioned diffusion cell [111].

In Chapter 7, physical quantities relevant for the design of slurry reactors are defined and reactor design equations will be given.
Moreover, the influence of the gas holdup, bubble size and particle size and concentration on the gas absorption rate will be treated in more detail.

CHAPTER 2

HYDRODYNAMIC BEHAVIOUR OF A BUBBLE COLUMN AND A SLURRY COLUMN

2.1. Introduction.

Gas-liquid contacting is of great importance in a number of industrial applications. In chemical processing, a gas-agitated contactor is often used to bring gas and liquid into intimate contact. When gas and liquid have been brought together, mass transfer takes place, which can be followed by a chemical reaction in the liquid phase.

In its simplest form, the gas-liquid contactor is a vertical vessel partially filled with liquid, having a gas disperser at the bottom. Its characteristic feature is that it has no mechanical stirrer or other moving parts. Inlet gas having a controlled superficial velocity is dispersed through the sparger into the liquid. At the top, gas and liquid are disengaged at an interface which must be controlled in a continuous operation. There may be a continuous liquid flow through the vessel, either co-current or counter-current relative to the gas flow. Generally, the superficial liquid velocity is relatively small in comparison with the superficial gas velocity. Gas-agitated contactors may be used as absorbers and strippers and are well-known as bubble columns.

This method of contacting a gas and a liquid is, probably, of still greater importance in catalytic processes. In these reaction systems a finely divided catalyst is kept in suspension in the liquid medium. On the active sites of the catalyst, a chemical reaction takes place between two components. One component is absorbed from the dispersed gas phase, the other is present as a pure liquid or has been dissolved in the liquid medium. Here, the reaction system is better known as a slurry reactor.

In slurry reactors the most important factor for gas-liquid contacting is the rate of gas absorption, which is proportional to the product of the overall mass transfer coefficient, K_L, and the specific interfacial area, a.

Mass transfer resistance in the gas phase is mostly negligible compared with that in the liquid phase, so, the rate of gas absorption can be given by k_La, where k_L is the liquid-film mass transfer coefficient.

Calderbank and Moo-Young [37] reported that for mass transfer from a dispersed gas phase k_L depends only on the physical properties of the system used and is independent of the operating conditions. Towell et al. [38] attributed most of the increase in k_La to the increase in interfacial area with the increasing superficial gas velocity. In their review on mass transfer in gas-liquid systems, Sideman et al. [39] came to the same conclusion.

Akita and Yoshida [40] found that k_L is directly proportional to the square root of the mean bubble diameter. The influence of the process conditions on the value of k_L remains limited, since the mean bubble diameter is almost independent of the superficial gas velocity for a given gas-liquid system.

Therefore, it can be concluded that for a given gas-liquid system in a given bubble column, k_L is almost independent of the superficial gas velocity and the superficial liquid velocity i.e. of the conditions under which the column is operated. The value of k_L is mainly determined by the physical properties of the system used. Its contribution to the increase of the rate of gas absorption at increasing superficial gas velocity is almost negligible. The increasing rate of gas absorption at higher values of the superficial gas velocity is mainly due to the increase of the specific interfacial area.

For a given system, the value of the specific interfacial area is dependent on the Sauter mean bubble diameter and the gas holdup.

They can be affected by the following system properties and process conditions:

- transport properties of gas and liquid;
- concentration of electrolytes;
- concentration of solid particles;
- type and position of gas distributor and orifice diameter;

- dimensions and geometry of the column;
- superficial gas velocity;
- superficial liquid velocity;
- presence and dimensions of internal devices.

In this chapter, we discuss the influence of some of the system properties and process conditions on the gas holdup and Sauter mean bubble diameter and, as a consequence, on the value of the specific interfacial area.
In all our experiments, the following properties and conditions are identical:
- the physical properties of the gas;
- dimensions and geometry of the gas distributor;
- diameter of the column.
- the superficial liquid velocity, which was zero.

Sometimes, the presence of internal devices is unavoidable in performing the measurements.

2.2. Physical quantities influencing mass transfer.

2.2.1. Average gas holdup.

When gas is continuously bubbled through a deep liquid, a certain volume of liquid will be displaced by an equal volume of the dispersed gas phase. The amount of gas can be expressed by the volume fraction of gas or gas holdup in the dispersion:

$$\varepsilon_{av} = V_G/(V_L + V_G) \qquad (2\text{-}1)$$

If the cross-sectional area of the column is constant along the height of the dispersion, this quantity can be calculated from the height of the dispersion H_D, and the clear liquid height H_0:

$$\varepsilon_{av} = (H_D - H_0)/H_D \qquad (2\text{-}2)$$

With eqn (2-1) or (2-2), it is possible to calculate an average gas holdup in the dispersion.
For a given column, the average gas holdup is commonly given as a function of the superficial gas velocity, defined by:

$$u_G = \Phi/A \qquad (2\text{-}3)$$

According to the work of Towell et al. [38] and Reith et al. [41,42], data on gas holdup can be correlated by:

$$v_r = v_o + bu_G \qquad (2\text{-}4)$$

where v_o is the terminal velocity of a single bubble and $b = 2$.
The left term of eqn (2-4) is known as the slip or relative velocity. For <u>cocurrent</u> flow of gas and liquid:

$$v_r = u_G/\varepsilon_{av} - u_L/(1 - \varepsilon_{av}) \qquad (2\text{-}5a)$$

For <u>countercurrent</u> flow of gas and liquid:

$$v_r = u_G/\varepsilon_{av} + u_L/(1 - \varepsilon_{av}) \qquad (2\text{-}5b)$$

In the present work, the superficial liquid velocity u_L equals 0.
One of the consequences of eqn (2-4) is that a limit of gas holdup will be reached for high values of the superficial gas velocity. Combination of eqns (2-4) and (2-5a) or (2-5b) gives:

$$1/\varepsilon_{av} = b + v_o/u_G = 1/\varepsilon_\infty + v_o/u_G \qquad (2\text{-}6)$$

so that for $u_G \to \infty$ the limiting value of the average gas holdup, denoted as ε_∞, will be $1/b$. Since $\varepsilon_\infty \leq 1$, it follows:

$$b \geq 1 \qquad (2\text{-}7)$$

At low values of u_G, eqn (2-6) yields:

$$\varepsilon_{av} = u_G/v_o \qquad (2\text{-}8)$$

Correlation (2-8) holds for $u_G \leq 3$ cm s^{-1} [9,10,39,43].
A large number of other correlations on gas holdup as a function of superficial gas velocity have been proposed [10,43-52]. Most of these correlations contain one or more dimensionless groups which in turn consist of physical quantities of the dispersed and continuous phase.
Some correlations cannot be used to describe the gas holdup presented in this study because these correlations have been obtained from experiments performed in smaller columns or in a different range of superficial gas velocities. It is known that identical superficial gas velocities in smaller columns, $T \leq 15$ cm, lead to higher values of the gas holdup [9,39,43,52-55].
In Table 2.1., correlations for gas holdup in bubble columns are summarized. Correlations mentioned in Table 2.1. have been obtained from experiments in large-diameter columns, $T > 15$ cm, and in a range of superficial gas velocities, $u_G > 3$ cm s^{-1}.

With respect to the average gas holdup, we have investigated the influence of the following physical properties and process conditions:
- clear liquid height;
- concentration of electrolytes;
- concentration of solid particles;
- superficial gas velocity.

The effect of the clear liquid height on the average gas holdup was found to be negligible by Yoshida and Akita whereas Gestrich and Rähse [51] reported that any influence can be neglected for clear liquid heights above 2 m. Several investigators [43,50,53] have observed that the gas holdup in aqueous electrolyte solutions is slightly larger than that in pure liquids or non-electrolyte solutions, whereas Van Dierendonck [9] did not find any influence of addition of electrolytes on the gas holdup.
The effect of the superficial gas velocity on the average gas holdup has been discussed above and can be found from the correlations of Table 2.1.
In the present study, the influence of porous activated carbon particles, up to a solids concentration of about 12 kg m^{-3}, on the average gas holdup has been investigated. Not only for the air-water system, but also for an electrolyte solution.

2.2.2. Gas-holdup distribution.
In the preceding section, the average gas holdup has been discussed. However, a non-homogeneous distribution of the gas holdup may be expected, considering the fact that in the dispersion three zones can be distinguished, each with its own specific properties.
In Fig. 2.1., these zones are drawn in a bubble column. First, one can locate a region near the gas distributor, where gas is dispersed into the liquid, the so-called on-stream zone. Secondly, near the surface where gas and liquid are disengaged, there can exist a foam layer with a relatively high gas holdup. Both the on-stream zone [38,42] and the foam layer [11] have a height of about 1-2 times the column diameter. Between these, a third region exists, sometimes called middle section. The properties of the on-stream zone and foam layer will not be influenced by the clear liquid height. The middle section, on the

Table 2.1. Correlations for gas holdup in bubble columns.

1. Towell et al. [38], Reith et al. [41,42]

$$\varepsilon_{av} = u_G/(v_o + 2u_G) \qquad (2\text{-}9)$$

Towell et al.:
$0 < u_G/(m\ s^{-1}) < 0.3$
$0 < u_L/(m\ s^{-1}) < 0.015$
$T = 0.4$ m and 1.05 m
$3.8 < H_0/T < 6.7$
water-air

Reith et al.:
$0.03 < u_G/(m\ s^{-1}) < 0.47$
$u_L = 0.021$ m s^{-1}
$T = 0.14$ m and 0.29 m
$5.6 < H_0/T < 27.1$
water-air
NaCl aq. soln-air

2. Van Dierendonck et al. [9,10]

$$\varepsilon_{av} = 1.2(\eta_L u_G/\sigma)^{3/4}\ Mo^{1/8} \quad \text{where } Mo = \sigma^3\rho_L/(\eta_L^4 g) \qquad (2\text{-}10)$$

$\varepsilon_{av} < 0.45$
$0.03 < u_G/(m\ s^{-1}) < 0.4$
$u_L < 0.02$ m s^{-1}
$T > 0.15$ m

$0.3 < H_0/T < 3$
$5\ 10^{-4} < \eta_L/(Pa\ s) < 5\ 10^{-3}$
$20\ 10^{-3} < \sigma/(N\ m^{-1}) < 75\ 10^{-3}$
$0.7\ 10^{3} < \rho_L/(kg\ m^{-3}) < 1.3\ 10^{3}$

3. Hughmark [44]

$$\varepsilon_{av} = (2 + (C_1/u_G)(\rho_L\sigma/C_2)^{1/3})^{-1} \quad \text{where } C_1 = 0.35 \text{ m s}^{-1} \text{ and } C_2 = 72 \text{ kg}^2\text{ m}^{-3}\text{ s}^{-2} \qquad (2\text{-}11)$$

$0.004 < u_G/(m\ s^{-1}) < 0.45$
$T > 0.1$ m

$0.9\ 10^{-3} < \eta_L/(Pa\ s) < 152\ 10^{-3}$
$25\ 10^{-3} < \sigma/(N\ m^{-1}) < 76\ 10^{-3}$
$0.78\ 10^{3} < \rho_L/(kg\ m^{-3}) < 1.7\ 10^{3}$

4. Akita et al. [43]

$$\frac{\varepsilon_{av}}{(1-\varepsilon_{av})^4} = C_3\left(\frac{T^2\rho_L g}{\sigma}\right)^{1/8}\left(\frac{T^3\rho_L{}^2 g}{\eta_L{}^2}\right)^{1/12}\left(\frac{u_G}{(Tg)^{1/2}}\right) = C_3 M^{1/24} Ca \qquad (2\text{-}12)$$

with $C_3 = 0.2$ for pure liquids and non-electrolyte solutions
and $C_3 = 0.25$ for electrolyte solutions

$0.005 < u_G/(m\ s^{-1}) < 0.42$
$T = 0.15$ m, 0.3 m and 0.6 m

$0.58\ 10^{-3} < \eta_L/(Pa\ s) < 21.1\ 10^{-3}$
$22.3\ 10^{-3} < \sigma/(N\ m^{-1}) < 74.2\ 10^{-3}$
$0.79\ 10^{3} < \rho_L/(kg\ m^{-3}) < 1.59\ 10^{3}$

5. Mersmann [45]

$$\frac{\varepsilon_{av}}{(1-\varepsilon_{av})^4} = C_4\ u_G\left(\frac{\rho_L{}^2}{\sigma\Delta\rho g}\right)^{1/4}\left(\frac{\rho_L{}^2\sigma^3}{\eta_L{}^4\Delta\rho g}\right)^{1/24}\left(\frac{\rho_L}{\rho_G}\right)^{5/72}\left(\frac{\rho_L}{\Delta\rho}\right)^{1/3} \qquad (2\text{-}13)$$

semi-theoretical equation where $C_4 = 0.14$ m^{-1} s

other hand, will be larger with larger clear liquid heights [38]. In general, the gas holdup is somewhat lower in the on-stream zone and much higher in the foam layer with respect to the average gas holdup in the column. The average gas holdup can be obtained from:

$$\varepsilon_{av} = (1/V_D) \int_0^R \int_0^{2\pi} \int_0^{H_D} \varepsilon(r,\theta,z) \; r\,dr\,d\theta\,dz \qquad (2\text{-}14)$$

Because of the cylindrical geometry of both the vessel and the gas distributor, the local time-averaged gas holdup will be independent of θ:

$$\varepsilon_{av} = (2\pi/V_D) \int_0^R \int_0^{H_D} \varepsilon(r,z) \; r\,dr\,dz \qquad (2\text{-}15)$$

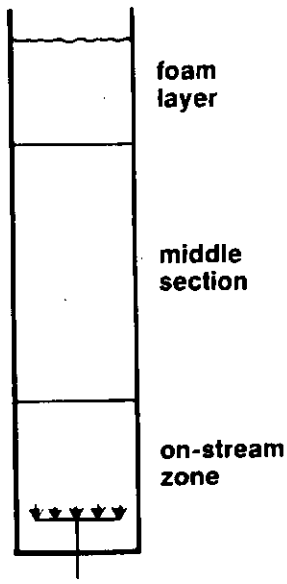

Fig. 2.1. Different zones in a bubble column.

Measurements of the radial gas holdup distribution have been carried out with a resistivity probe by Neal and Bankoff [56], Hills [57], Koide et al. [58] and Kojima et al. [59]. This probe gives two values of the cell current corresponding to two possible values of the gas holdup at the tip of the probe: zero if the point is in the liquid phase and unity if it is in the gas phase. The average local gas holdup is now calculated by integrating the output signal over a sampling period and dividing by the duration of the sampling period:

$$\varepsilon(r,z) = (1/t') \int_0^{t'} \varepsilon(r,z,t)\,dt \qquad (2\text{-}16)$$

With this resistivity probe, a parabolic distribution function of the local gas holdup as a function of the column radius has been found in small columns.

Reith et al. [42] measured axial and radial gas holdup distributions by means of manometer tubes placed at different longitudinal and radial distances in the column. No radial pressure gradients could be detected.
In the present study, we measured also the local gas holdup by means of manometer tubes. The local gas holdup was determined as a function of:
- the axial and radial distance in the dispersion;
- superficial gas velocity;
- presence and concentration of solid particles.

2.2.3. Solid particle distribution.
On the analogy of section 2.2.2, identical remarks can be made with respect to the local solids concentration in the case that solid particles are added to the dispersion. In bubble columns, a non-uniform distribution of the solid particles may occur due to sedimentation. Therefore, the average solids concentration can be given by:

$$\bar{C}_p = (1/V_D) \int_0^R \int_0^{2\pi} \int_0^{H_D} C_p(r,\theta,z)\, r\, dr\, d\theta\, dz \qquad (2\text{-}17)$$

For reasons mentioned in section 2.2.2., this eqn (2-17) can be simplified:

$$\bar{C}_p = (2\pi/V_D) \int_0^R \int_0^{H_D} C_p(r,z)\, r\, dr\, dz \qquad (2\text{-}18)$$

It can be shown that small solid particles are well suspended in the dispersion of a bubble column.
The minimum liquid velocity required to keep a small particle ($Re_p < 1$) in suspension, can be calculated according to Stokes' law:

$$v_\infty = d_p^2(\rho_p - \rho_L)g/(18\eta_L) \qquad (2\text{-}19)$$

The density ρ_p is the density of the porous catalyst particle, totally filled with liquid:

$$\rho_p = (1 - \varepsilon_p)\rho_s + \varepsilon_p\rho_L \qquad (2\text{-}20)$$

For a 10 wt % Pd/C catalyst, common values are:

$$d_p = 4\ 10^{-6}\ m;\ \varepsilon_p = 0.8;\ \rho_s = 2\ 10^3\ kg\ m^{-3} \qquad (2\text{-}21)$$

When the liquid used is water, eqn (2-19) becomes

$$v_\infty = 2\ 10^{-6}\ m\ s^{-1} \qquad (2\text{-}22)$$

whereas the Reynolds number, based on the diameter of the particle, equals:

$$Re_p = \rho_L d_p v_\infty/\eta_L = 8\ 10^{-6} \qquad (2\text{-}23)$$

Thus the assumption of creeping flow around the solid particle is justified. As long as the particles do not interfere with one another, this calculation holds. It is plausible that the vertical liquid velocity component will be more than $2\ 10^{-6}\ m\ s^{-1}$, even at low values of the superficial gas velocity. Imafuku et al. [60] observed that the velocity needed to keep small particles in a homogeneous suspension depends only slightly on the total amount of solid particles within the column, which is in agreement with the above-mentioned result.

For the determination of the solids holdup, three methods are available:
- visual observation;
- pressure drop measurement;
- analysis of samples taken from the suspension.

Because of the relatively low catalyst concentration used in this work and the opacity of the dispersion caused by the carbon particles, we used the latter method.
With respect to the calculation of gas holdup in slurry systems, it can be assumed that the contribution of the porous solid particles to the volume of the dispersion is negligible. For a solids concentration of 12 kg m^{-3}, the contribution of the solid part of the catalyst particle to the dispersion volume is only 0.6 percent.
Therefore, the expression given in eqn (2-1) can be used to calculate the average gas holdup for the slurry systems used in the present study.

2.2.4. Axial liquid-phase velocity distribution.
According to some investigators [56,57,61-64], a recirculation flow is initiated and propagated by a density difference in the column between the dispersion at the centre of the column and that near the wall. Owing to a higher gas holdup at the centre of the column, liquid is flowing upwards at the centre of the column and downwards near the wall.The radial gas holdup distribution is then approximated by [61]:

$$\varepsilon(r) = \langle\varepsilon\rangle((n + 2)/n)(1 - (r/R)^n) \qquad (2\text{-}24)$$

where $\langle\varepsilon\rangle$ is the average gas holdup of the cross-sectional area at a certain axial height in the dispersion. Mostly a value of $n = 2$ is taken.
However, the proof is not convincing, for:
- most of the experimental proof has been obtained from experiments in small diameter columns where by coalescence of gas bubbles above the gas distributor some very large cigar-shaped bubbles are formed;
- the experimental proof is not consistent. Using the resistivity probe technique, Koide et al. [58] found an almost flat radial gas holdup distribution throughout the cross-sectional area of a 5.5 m diameter column, whereas they observed a liquid recirculation flow with a cylindrical symmetry;
- if a uniform radial gas holdup distribution is assumed in a bubble column, no recirculation pattern and hence no axial liquid velocity distribution should be found. However, it can easily be shown that also an axial liquid velocity distribution will occur even though the gas holdup has been distributed uniformly throughout the dispersion.

To show this, the following assumptions are made:
- all the time-averaged liquid velocity components, except in axial direction, equal zero:

$$\bar{v}_r = 0;\ \bar{v}_\theta = 0;\ \bar{v}_z \neq 0 \qquad (2\text{-}25)$$

- near the wall, there is a thin layer filled with a dispersion having a density ρ ranging from:

$$\rho_d \leq \rho \leq \rho_L \quad \text{for} \quad R_d \leq r \leq R \qquad (2\text{-}26)$$

- within this layer, there is a core with a <u>uniform</u> gas-liquid dispersion:

$$\rho = \rho_d \quad \text{for} \quad 0 \leq r \leq R_d \qquad (2\text{-}27)$$

- the liquid velocity at the wall should be zero:

$$\bar{v}_z(R) = 0 \qquad (2\text{-}28)$$

- because the layer near the wall is so thin relative to the diameter of the column ($R_d \approx R$), it is assumed that the velocity near the wall is that of the periphery of the core:

$$\bar{v}_z(R_d) = \bar{v}_w \tag{2-29}$$

In Fig. 2.2., these dimensions and velocities have been clarified for a bubble column.
The superficial liquid velocity is given by:

$$\int_0^R \int_0^{2\pi} \bar{v}_z(r,\theta)\, r\, dr\, d\theta = u_L A \tag{2-30}$$

Assuming a cylindrical-symmetrical velocity profile for the liquid phase, based on the cylindrical geometry of both the column and the gas distributor, eqn (2-30) reads:

$$u_L = (2/R^2) \int_0^R \bar{v}_z(r)\, r\, dr \tag{2-31}$$

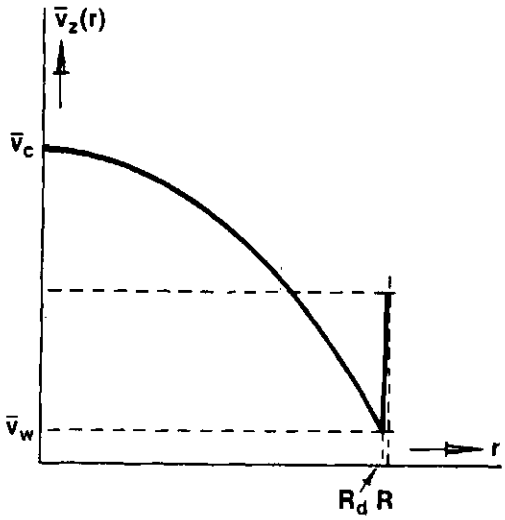

Fig. 2.2. Axial liquid velocity profile in a bubble column.

The equation of motion for the axial direction reads:

$$(1/r)d(r\tau_{rz})/dr = -dp/dz - \rho g \tag{2-32}$$

This equation of motion can be integrated for the core with a radius R_d with the boundary condition:

$$\tau_{rz} = 0 \text{ for } r = 0 \tag{2-33}$$

assuming constant density of the core:

$$\rho = \rho_d \text{ for } 0 \leq r \leq R_d \tag{2-34}$$

The following solution is then found:

$$\tau_{rz} = -(dp/dz + \rho_d g)r/2 \quad \text{with} \quad 0 \leq r \leq R_d \tag{2-35}$$

A relation between the shear stress at the wall and the pressure gradient can now be found:

$$\tau_w = -(dp/dz + \rho_d g)R/2 \tag{2-36}$$

The axial liquid velocity can be found if the shear stress may be approximated by the following equation:

$$\tau_{rz} = -\rho_d \nu_t \, d\bar{v}_z/dr \tag{2-37}$$

In general, the turbulent viscosity ν_t is a function of position in the column. In this model, it has been assumed that the turbulent viscosity is constant over the core at the same axial position in the dispersion.
From eqns (2-35) and (2-37), it follows:

$$\rho_d \nu_t \, d\bar{v}_z/dr = (dp/dz + \rho_d g)r/2 \tag{2-38}$$

Integration of eqn (2-38) yields:

$$\bar{v}_z(r) = \tfrac{1}{4}r^2(dp/dz + \rho_d g)/(\rho_d \nu_t) + C_5 \tag{2-39}$$

In the present study, the superficial liquid velocity equals zero:

$$u_L = 0 = (2/R^2)\int_0^R \bar{v}_z(r)\, r\,dr \tag{2-40}$$

from which it follows that:

$$C_5 = -R^2(dp/dz + \rho_d g)/(8\rho_d \nu_t) \tag{2-41}$$

The axial liquid velocity distribution is then given by:

$$\bar{v}_z(r) = \{(r/R)^2 - \tfrac{1}{2}\}(dp/dz + \rho_d g)R^2/(4\rho_d \nu_t) \tag{2-42}$$

For $r = R_d$ we find:

$$\bar{v}_z(R_d) = \bar{v}_w = (dp/dz + \rho_d g)R_d^2/(8\rho_d \nu_t) \tag{2-43}$$

Since $R_d \approx R$, we approximately obtain:

$$\bar{v}_z(r) = 2\bar{v}_w\{(r/R)^2 - \tfrac{1}{2}\} \tag{2-44}$$

The same result is obtained after introducing $(\langle\varepsilon\rangle - \varepsilon(r)) = 0$ for $0 \leq r \leq R$ into eqn (12) of the work of Ueyama and Miyauchi [61].
The eqn (2-44) makes clear that the time-averaged axial liquid velocity equals zero for:

$$r/R \approx 0.71 \tag{2-45}$$

which is in good agreement with values found in the theoretical and experimental work of other investigators [57-59,61,62,64].
Furthermore, it follows that the axial liquid velocity at the centre of the column has a value identical to that near the wall but with opposite sign:

$$\bar{v}_c = -\bar{v}_w \tag{2-46}$$

Some liquid velocity data taken from literature are plotted in Fig. 2.3. The values of $\bar{v}_w$ have been calculated by means of the least-squares method. The agreement between this model and the experimental values given by Pavlov [65] and those from Yamagoshi [66] is good. From this agreement it can be concluded that the proposed model holds very well for superficial gas velocities from about 5 to 17 cm s^{-1} and column diameters from 17 to 25 cm.
In this study, we have measured the axial liquid velocity in the air-water system with a column diameter of 29 cm and superficial gas velocities from 2 to 29 cm s^{-1}.

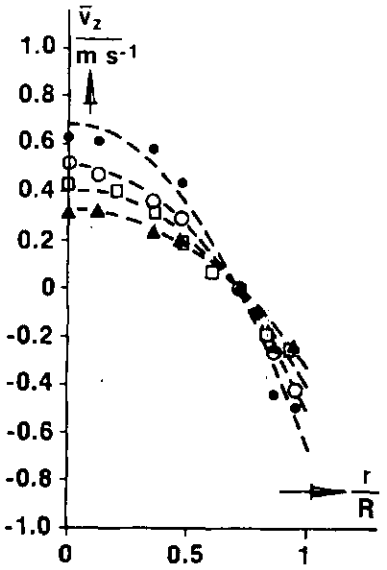

Pavlov data [65]

$u_G/(m\ s^{-1})$	$\bar{v}_w/(m\ s^{-1})$
▲ 0.05	-0.33
○ 0.10	-0.51
● 0.17	-0.68

Yamagoshi data [66]

$u_G/(m\ s^{-1})$	$\bar{v}_w/(m\ s^{-1})$
□ 0.05	-0.41

Fig. 2.3. Comparison of the proposed model for axial liquid velocity distribution with literature data. The broken lines represent eqn (2-44).

2.2.5. Sauter mean gas bubble diameter.
Generally, in industrial bubble columns high values of the superficial gas velocity are applied. In that case the same three zones can be distinghuished with respect to the bubble diameter as were discussed in section 2.2.2.
In the on-stream zone, the gas bubble diameter is determined by the sparger performance and depends on the gas velocity in the orifice and the orifice diameter.
These initial gas bubbles, i.e. the gas bubbles in the on-stream zone, are different in size from the bubbles rising through the middle section of the column. In the region near the sparger, the bubble diameter is independent of the physical properties of the system and can be calculated from [40]:

$$d_{si}/d_o = 1.88\ (Fr_{or})^{1/3} \qquad (2\text{-}47)$$

In the foam layer, no separate gas bubbles can be distinguished. Compartments of gas are separated from each other by very thin layers of liquid and consequently, the gas holdup will be higher than that in the on-stream zone or the middle section and can even approximate unity.

In the middle section, the properties of the dispersion are governed by the gas superficial gas velocity and are independent of the type of sparger or sparger performance [10,38]. The ultimate bubble diameter depends primarily on the turbulence in the continuous phase [38,39]. Because the middle section usually forms the major part of the dispersion, the discussion is limited here to this zone.
In the dispersion, a distribution of bubble sizes occurs. When the density function is $f(d_b)$, the n^{th} moment μ_n of the distribution is defined by:

$$\mu_n \equiv \int_0^\infty d_b^n \, f(d_b) \, d(d_b) \tag{2-48}$$

It is usual to calculate the so-called Sauter mean bubble diameter, defined by:

$$d_s \equiv \mu_3/\mu_2 \tag{2-49}$$

The gas bubble diameters can be grouped into classes, each with a lower and an upper diameter limit. The Sauter mean bubble diameter is then given by:

$$d_s = \sum_i n_i d_i^3 \; / \; \sum_i n_i d_i^2 \tag{2-50}$$

where d_i is the arithmetic mean diameter of a bubble of class i.
The maximum stable bubble diameter in a bubble column filled with a low-viscous liquid is given by the balance of surface tension force and buoyancy force:

$$d_{max}\pi\sigma = d_{max}^3 \pi g(\rho_L - \rho_G)/6 \tag{2-51}$$

Experiments yield a somewhat higher value [45] than eqn (2-51):

$$d_{max} \approx 3(\sigma/(\rho_L - \rho_G)g)^{\frac{1}{2}} \tag{2-52}$$

For low-viscous liquids ($\eta_L < 3$ mPa s), the Sauter mean bubble diameter can be approximated by:

$$d_s \approx 1.8(\sigma/(\rho_L - \rho_G)g)^{\frac{1}{2}} \tag{2-53}$$

Further expressions to calculate the Sauter mean diameter have been published in the literature [9,10,40,45] and are listed in Table 2.2.
In this work, we have determined the Sauter mean gas bubble diameter as a function of:
- the superficial gas velocity;
- concentration of electrolyte;
- concentration of solid particles;
- clear liquid height.

The other correlations mentioned in Table 2.2., except Mersmann's correlation, give a smaller mean bubble diameter with increasing superficial gas velocity. It can be calculated from correlations of Van Dierendonck et al. that the mean gas bubble diameter in aqueous electrolyte solutions is much smaller than in pure water because of the change in dynamic surface tension and the electrostatic potential of the resultant ions at the gas-liquid interface [9,10].
For measuring the bubble diameter, four methods can be used:
- chemical method [9,41,49];
- photographic method [9,38,40,41];
- resistivity probe method [56,57];
- gas disengagement method [67].

With the chemical method, one can only obtain the mean bubble diameter of the

Table 2.2. Correlations for the Sauter mean bubble diameter in bubble columns.

1. Akita and Yoshida [40]

$$d_s = 26\ T\ Bo^{-0.5}\ Ga^{-0.12}\ Fr^{-0.12} \qquad (2\text{-}54)$$

T = 7.7 cm, 15 cm and 30 cm
$u_G \leq 0.04$ m s^{-1}

$0.79\ 10^3 \leq \rho_L/(\text{kg m}^{-3}) \leq 1.17\ 10^3$
$0.58\ 10^{-3} \leq \eta_L/(\text{Pa s}) \leq 21.1\ 10^{-3}$
$22.3\ 10^{-3} \leq \sigma/(\text{N m}^{-1}) \leq 74.2\ 10^{-3}$

2. Mersmann [45]

$$d_s \simeq 1.8(\sigma/(\rho_L - \rho_G)g)^{\frac{1}{2}} \qquad \text{for } \eta_L \leq 3\ 10^{-3}\ \text{Pa s} \qquad (2\text{-}55)$$

3. Van Dierendonck et al. [9,10]

$$d_s^2 = C_6 \left(\frac{\sigma}{\rho_L g}\right) \left(\frac{\eta_L u_G}{\sigma}\right)^{-\frac{1}{2}} Mo^{-\frac{1}{4}} \qquad (2\text{-}56)$$

with C_6 = 6.25 for pure liquids
and C_6 = 2.1 for electrolyte solutions

$\varepsilon_{av} \leq 0.45$
$1 \leq H_D/T \leq 3$
$u_L \leq 0.03$ m s^{-1}
$T \geq 0.15$ m

$20\ 10^{-3} \leq \sigma/(\text{N m}^{-1}) \leq 75\ 10^{-3}$
$1\ 10^{-3} \leq \eta_L/(\text{Pa s}) \leq 3\ 10^{-3}$
$0.03 \leq u_G/(\text{m s}^{-1}) \leq 0.3$

dispersion as a whole and no bubble diameter distribution. Furthermore, one has to add chemical components or a catalyst to the liquid, which may change the physical properties of the liquid and therewith may influence the value of the bubble diameter.
Another disadvantage of the chemical method is the fact that one has to know the kinetics of the chemical reaction between the component dissolved in the liquid phase and the absorbed component from the gas phase.
The photographic method and the resistivity probe method have the advantage that they can be used at any position in the dispersion to give a local gas bubble diameter distribution. However, when taking pictures from outside the column, only a small layer of dispersion can be studied. This means that the column must have a sight glass or must be made up of a transparant material.

To measure bubble diameter distributions in the dispersion away from the wall, one has to use an introscope. In this case, and also when a resistivity probe is used, it has to be assumed that the presence of the introscope or probe does not influence the local bubble diameter distribution. Measurements by Van Dierendonck et al. [10] showed that there was no difference between the values of the mean bubble diameter calculated from pictures taken near the wall and determined from pictures taken at the centre of the column.
Recently, Sriram and Mann [67] introduced the dynamic gas disengagement technique for measuring the bubble diameter distribution. This method, which will be developed further in section 2.2.7., is employed for the determination of the mean bubble diameter of the gas bubbles in slurry columns where the presence of the catalyst particles makes it impossible to take pictures.

2.2.6. Specific interfacial area.
Mass transfer in a given system is primarily governed by the value of the interfacial area, i.e. the value of the gas bubble surface per unit volume of the reaction system:

$$a = A_t/V_D \qquad (2\text{-}57)$$

from which it can be deduced that:

$$a = 6\epsilon_{av}/d_s \qquad (2\text{-}58)$$

The value of the specific interfacial area can now be calculated from the correlations given in sections 2.2.1. and 2.2.5., respectively. As a consequence, the influence of the physical properties and the process conditions on the value of the specific interfacial area can be derived from the influence of these properties and conditions on the average gas holdup and the Sauter mean bubble diameter separately.
For a given reaction system, the specific interfacial area is only dependent on the average gas holdup because the Sauter mean bubble diameter is almost constant for $u_G > 3$ cm s^{-1}. In Table 2.3., correlations for the specific interfacial area in bubble columns are given.
Akita and Yoshida [40] as well as Reith and Beek [41] found an increase of the specific interfacial area with increasing column diameter. According to Akita and Yoshida, this increase is due mainly to the decrease of d_s with increasing column diameter.
Obviously, the value of the specific interfacial area will increase with a higher superficial gas velocity owing to the increase of the average gas holdup.
The value of the specific interfacial area can be determined by two methods:
- fast chemical reaction technique;
- experimental determination of average gas holdup and Sauter mean bubble diameter.

In the foregoing section, both methods were discussed.
In section 2.5.6., we have calculated the value of the specific interfacial area from the values of the average gas holdup and the Sauter mean bubble diameter.

2.2.7. Dynamic gas disengagement.
In section 2.2.5., we discussed some methods to determine the gas bubble diameter distribution and the specific interfacial area of the gas bubbles in the dispersion. One of the methods is that of taking pictures of the gas bubbles in the dispersion, counting the bubbles and classifying them according to their diameter to calculate the Sauter mean diameter. However, this technique could not be applied successfully under the conditions we used in the slurry column because of the presence of the light-absorbing black particles. Therefore, a technique has been developed to determine the bubble diameter distribution by means of the dynamic gas disengagement method. This technique was introduced by Sriram and Mann [67]. They used the technique in a bubble column of 30 cm diameter with a superficial gas velocity of 2 cm s^{-1}, while Vermeer and Krishna [68] have recently used this method with superficial gas velocities of more than 0.3 m s^{-1}. Their column was only 19 cm in diameter, however.
In this section, a method is described to determine the specific interfacial area and the Sauter mean bubble diameter from the relation between the height of the dispersion and time after a sudden cut-off of the gas supply.
In developing this method, the following assumptions will be made:
- the gas bubble diameter distribution is the same throughout the dispersion;
- during the rising of the gas bubbles after the gas supply cut-off, bubble interactions do not change the initial diameter distribution, i.e.: the

Table 2.3. Correlations for the specific interfacial area in bubble columns.

1. Van Dierendonck et al. [9,10]

$$a = C_7(\eta_L u_G/\sigma)(\rho_L g/\sigma)^{\frac{1}{2}} M^{\frac{1}{4}} \qquad (2\text{-}59)$$

with $C_7 = 2$ for pure liquids
and $C_7 = 5$ for electrolyte solutions

$\varepsilon_{av} \leq 0.4$
$T \geq 0.15$ m
$u_L \leq 0.02$ m s^{-1}
$1 \leq H_0/T \leq 3$

$20\ 10^{-3} \leq \sigma/(\text{N m}^{-1}) \leq 75\ 10^{-3}$
$1\ 10^{-3} \leq \eta_L/(\text{Pa s}) \leq 3\ 10^{-3}$
$0.03 \leq u_G/(\text{m s}^{-1}) \leq 0.3$

2. Yoshida and Akita [43]

$$a = 0.6\ Sc^{0.5}\ Bo^{0.62}\ Ga^{0.31}\ Sh^{-1}\ T^{-1}\ \varepsilon_{av}^{1.1} \qquad (2\text{-}60)$$

$T = 0.15$ m, 0.3 m and 0.6 m
$0.005 \leq u_G/(\text{m s}^{-1}) \leq 0.42$

$0.79\ 10^3 \leq \rho_L/(\text{kg m}^{-3}) \leq 1.59\ 10^3$
$0.58\ 10^{-3} \leq \eta_L/(\text{Pa s}) \leq 21.1\ 10^{-3}$
$22.3\ 10^{-3} \leq \sigma/(\text{N m}^{-1}) \leq 74.2\ 10^{-3}$

processes of breaking-up and coalescence are in equilibrium with each other and the initial diameter distribution remains unchanged;
- after the gas supply cut-off, the gas bubbles have a velocity of rise which is a function of the bubble diameter.

In Fig. 2.4a., the stationary gas-liquid dispersion in a bubble column is represented. There is a range of bubble sizes which is uniform throughout the dispersion. The situation of Fig. 2.4a. can be transformed into the equivalent form of Fig. 2.4b. When the gas supply is cut off, the gas bubbles rise and disengage at the level of the dispersion. However, after a certain time, more of the large bubbles will have left the dispersion owing to their higher velocity of rise. This situation is given in Fig. 2.4c.

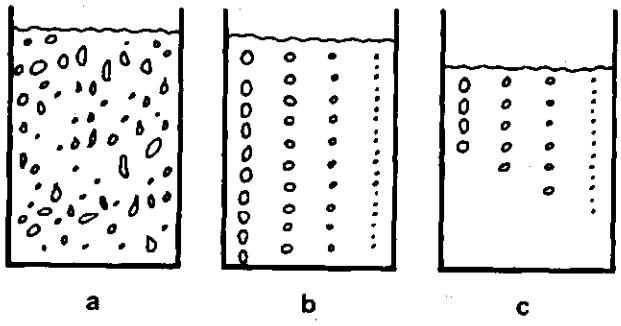

Fig. 2.4. Schematic representation of dynamic gas disengagement.

During disengagement the level of dispersion falls with respect to the vessel with a velocity which is a function of time:

$$v_s(t') = dH(t)/dt \Big|_{t=t'} \tag{2-61}$$

The origin of the axial coordinate H is at the bottom of the column. A gas bubble of diameter d_b has a velocity of rise v_d with respect to the vessel. The velocity of the gas bubble with respect to the level of the dispersion is:

$$v(t') = v_d - dH(t)/dt \Big|_{t=t'} \tag{2-62}$$

For the volume fraction distribution of the gas bubbles the following equation holds:

$$\int_0^\infty f_1(w)\, dw = 1 \tag{2-63}$$

Furthermore, note that at time $t = t'$, all bubbles with a velocity of rise

$$v_d > H(t')/t' \tag{2-64}$$

have left the dispersion.
At $t = 0$, the volume of gas in the dispersion is:

$$V_G(0) = (H_D - H_0)A \tag{2-65}$$

whereas at $t = t'$, the volume of gas in the dispersion is given by:

$$V_G(t') = (H(t') - H_0)A \tag{2-66}$$

so that the volume fraction of gas which has left the dispersion between $t = 0$ and $t = t'$ follows from:

$$\frac{V_G(0) - V_G(t')}{V_G(0)} = \frac{H_D - H(t')}{H_D - H_0} \tag{2-67}$$

At $t = t'$ all bubbles with a velocity of rise higher than $H(t')/t'$ have left the dispersion. Besides, a volume fraction $g(w)$ of the gas bubbles with a velocity of rise lower than $H(t')/t'$ has disengaged. Thus the volume fraction of gas which has left the dispersion is:

$$\Omega \equiv \frac{H_D - H(t')}{H_D - H_0} = \int_{v(t')}^\infty f_1(w)\, dw + \int_0^{v(t')} g(w) f_1(w)\, dw = \tag{2-68}$$

$$1 + \int_0^{F_1(v(t'))} g(w)\, dF_1(w) - F_1(v(t'))$$

The function $g(w)$ gives the volume fraction of gas bubbles with velocity of rise w which has left the dispersion at $t = t'$:

$$g(w) = \frac{\int_0^{t'} (w - dH(t)/dt)\, dt}{\int_0^{t_w} (w - dH(t)/dt)\, dt} \tag{2-69}$$

Here, t_w is that time at which all bubbles with velocity of rise w have

disengaged:

$$t_w = H_w/w \tag{2-70}$$

where H_w designates the height of the dispersion at t_w.
From eqn (2-69), it follows that:

$$g(w) = \frac{wt' + (H_D - H(t'))}{wt_w - H_w + H_D} \tag{2-71}$$

Using eqn (2-70), this result can be rewritten into:

$$g(w) = \frac{wt' + (H_D - H(t'))}{H_D} \tag{2-72}$$

Substitution of g(w) into eqn (2-68) gives, after rearrangement:

$$\frac{(H(t') - H_0)H_D}{H_D - H_0} = H(t') \int_0^{v(t')} f_1(w)\, dw - t' \int_0^{v(t')} w f_1(w)\, dw \tag{2-73}$$

from which $f_1(w)$ can be calculated if the relation between H and t' is known.
It is now assumed that there is a correlation between diameter and velocity of the gas bubbles, which means that the volume fraction $f_1(w)\, dw$ can be transformed into a volume fraction $f_2(d_b)\, d(d_b)$ as a function of the bubble diameter.
According to section 2.2.5., the Sauter mean bubble diameter is given by:

$$d_s = \mu_3/\mu_2 = \frac{\int_0^{\infty} d_b^3 f_2(d_b)/(\pi d_b^3/6)\, d(d_b)}{\int_0^{\infty} d_b^2 f_2(d_b)/(\pi d_b^3/6)\, d(d_b)} = \frac{1}{\int_0^{\infty} d_b^{-1} f_2(d_b)\, d(d_b)} \tag{2-74}$$

The specific interfacial area is given by:

$$a = 6\varepsilon_{av}/d_s \tag{2-75}$$

Knowledge of the relation between the diameter of the gas bubble and the velocity of rise is needed to determine the volume fraction distribution as a function of the bubble diameter.
A number of publications provide relevant data. The most simple relation is found when using the velocity of rise of a single spherical gas bubble in an infinitely extended liquid.
Marrucci [69] proposed a relation for the velocity of rise of a swarm of spherical bubbles based on the velocity of a single spherical bubble of the same diameter:

$$v_d = v_o\, (1 - \varepsilon)^2/(1 - \varepsilon^{5/3}) \tag{2-76}$$

In this study we have used the dynamic gas disengagement technique for determining the Sauter mean gas bubble diameter and the specific interfacial area in slurry systems, measured as a function of:
- the superficial gas velocity;
- the concentration of solid particles;
- the concentration of electrolytes.

The results for the Sauter mean diameter from pictures of the air-water system were compared with results of the gas disengagement technique in the same system to prove the applicability of this method.